

Investigating the Formation of a Repulsive Hydrogel of a Cationic 16mer Peptide at Low Ionic Strength in Water by Vibrational Spectroscopy and Rheology

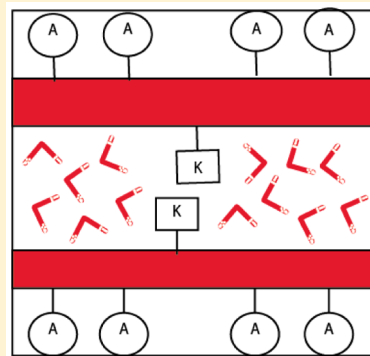
David DiGuiseppi,[†] Jodi Kraus,^{†,‡} Siobhan E. Toal,[§] Nicolas Alvarez,[‡] and Reinhard Schweitzer-Stenner^{*†}

[†]Department of Chemistry and [‡]Department of Chemical and Biological Engineering, Drexel University, 3141 Chestnut Street, Philadelphia, Pennsylvania 19104, United States

[§]Department of Chemistry, University of Pennsylvania, Philadelphia, Pennsylvania 19104, United States

S Supporting Information

ABSTRACT: The cationic peptide (AAKA)₄ (AK16) exhibits a high propensity for aggregation into β -sheet-like structures in spite of the high positive charge of its protonated lysine side chains. Upon incubation into an aqueous solution, the peptide maintains a metastable β -sheet-like structure with fibrillar content, the apparent stability of which increases with peptide concentration. In the presence of a sufficiently high concentration of anions, the peptide spontaneously forms a hydrogel at millimolar concentrations. Interestingly, we find that even in the absence of gel-supporting anions, the peptide is capable of forming a hydrogel in the centimolar range. Rheological data reveal that the gel is a stable elastic solid. These data show that the peptide can overcome the repulsive interactions between the positively charged ammonium groups of the lysine residues. The addition of 1 M NaCl just accelerates this process. Atomic force microscopy images of the peptide gel reveal fibrils with thicknesses between 4 and 8 nm, which suggests that they contain multiple layers of sheets. We propose that long tapes of β -sheet are arranged in fibrils via stacking of alternating interfaces induced by hydrophobic interactions between alanine side chains and by the formation of a hydrogen bonded water network between hydrophilic sides of AK16 β -sheets, which leads to the observed immobilization of the solvent in the formed hydrogel. Water immobilization is proposed as the likely cause for a significant increase in the amide I' oscillator strength of the formed β -sheet structures.



INTRODUCTION

The self-assembly of biomolecules is an important issue explored in biomedical, biophysical, and biomaterial research. Interest stems partly from the diverse supramolecular structures such as fibrils, ribbons, nanotubes, and monolayers formed by spontaneous self-assembly.¹ If peptides or proteins are used as building blocks, such higher order structures are predominantly formed as aggregates of β -sheet-type tapes.² Peptide and protein self-aggregation is implicated in a variety of diseases such as Alzheimer's disease, Parkinson's disease, Huntington's disease, prion-transmissible spongiform encephalopathies, and so-called polyalanine diseases, which all involve self-assembly of proteins into fibrils and insoluble plaques.³ With respect to biotechnology, the self-assembly capability of biomolecules has more positive aspects. It allows the generation of material with incorporated biocompatibility and biofunctionality, such as both ligand and metal recognition.⁴ Within this context, hydrogels, i.e. a self-assembled mixture of e.g. peptides and water, have garnered much interest for their potential use in tissue engineering and drug delivery.⁵

The parameters that govern peptide/protein aggregation in general and the formation of specific supramolecular structures like fibrils, nanotubes, and hydrogels in particular are still a

matter of debate.⁶ Many polypeptides that are intrinsically disordered in their monomeric state can self-aggregate into β -sheet suprastructures.⁷ However, only a limited number are capable of forming hydrogels. Several lines of evidence suggest that amphiphilicity is a necessary but insufficient requirement for a peptide's gelation in water.^{8–10} The strengths of hydrogels formed with amphiphilic peptides depend on the choice of residues for the hydrophobic and hydrophilic side, but the rheological properties do not always correlate with hydrophobicity.¹¹ Steric properties are of similar importance. On the hydrophilic site, the net charge should be small or zero in order to minimize electrostatic repulsion.⁸ Ideally, positively and negatively charged amino acid residues would alternate, as it is the case for the peptides with RADA,⁹ EMK,¹¹ VKVE,¹² IKIE, and FKFE^{13,14} repeats. Repeating sequences with more separated charges like (FE)₂(FK)₂ are also an option.¹³ All these peptides allow for hydrogen bonding and saltbridge formation between side chains of opposite charges. On the contrary, predominantly cationic or anionic amphiphilic

Received: August 1, 2016

Revised: August 30, 2016

Published: September 1, 2016

peptides are considered as poor gelators, since they can generally aggregate into gels only in the presence of counterions.^{12,13,15,16} Bowerman et al., for instance, investigated a series of Ac-(XKXK)-NH₂ peptides and found that (a) they require the addition of rather significant amounts of anions (in the submolar range) and that (b) the minimal anion concentration required for initiating aggregation and gelation decrease with increasing hydrophobicity of X on the hydrophobic site.¹⁷ All these observations are consistent with the notion that contrary to glasses, gels are always attractive.¹⁶

Recently Measey et al. reported that the highly cationic peptide AK16 (Ac-(AAKA)₄-NH₂) can form hydrogels at millimolar concentrations and acidic pH or high NaCl concentration.¹⁸ This is *per se* still in line with observations made for other highly cationic peptides (*vide supra*),^{12,13} even though one would not be inclined to classify this peptide as an ideal gelator owing to the comparatively low hydrophobicity of alanine.¹⁹ However, it is very surprising that even in the absence of counterions, AK16 can still form soluble aggregates with an antiparallel β -sheet structure.²⁰ The aggregation process for AK16 differs from the classical behavior of self-aggregating peptides. There is no initial nucleation phase in which peptides first form amorphous aggregates that over time convert into a more ordered nucleus of β -sheet structures.³ Below a certain threshold concentration,²⁰ the β -sheet structure, pre-existing in the solid state of AK16, dissociates only very slowly into amorphous aggregates. The initial amount of β -sheet aggregates varies somewhat in purchased solid-state batches. Above this critical concentration, the β -sheet aggregates did not dissociate on the time scale investigated by the authors (i.e., 2–3 h). This behavior is peculiar and defies the expectation that the charged side chains should facilitate the peptide's dissolution and very fast disaggregation into monomers in water. Molecular dynamics simulations revealed that AK16 can form thermally unstable antiparallel β -sheet structures in water.²¹ In the obtained conformation, Coulomb interactions are minimized since the protonated lysine side chains of adjacent strands point in opposite directions. However, one would expect that for such conformations of AK16 aggregates the formation of ribbons and the intertwining of fibrils would be inhibited by strong repulsive Coulomb interactions.

The examples listed above explicitly show that the influence of electrostatic interactions on peptide aggregation is not fully understood. We therefore wondered whether the alleged prohibitive influence of electrostatic repulsion on peptide gelation might not be able to inhibit the gelation of AK16 at a sufficiently high peptide concentration even in the absence of neutralizing anions. Therefore, we extended our investigation of AK16 in water into a peptide concentration regime above 10 mg/mL, which lies above the concentrations for which Measey et al. observed aggregation without gelation.²⁰ To this end we first measured the IR spectrum of samples with different concentrations of AK16 at and above 10 mg/mL in D₂O over a period of 5 days (one spectrum per day) to probe changes of the aggregation status. In parallel, we checked whether stock solution from where we took our samples had gelled. Thus, we observed gelation of a 20 mg/mL sample after 5 days. We characterized the gelled sample with atomic force microscopy. In a second step, we combined rheology with IR-spectroscopy to probe the kinetics of the gelation process of another 20 mg/mL sample in the absence and presence of submolar NaCl. Our data suggest that the addition of counterions accelerates the gelation process, as expected. The rheology data revealed the

formation of an elastic gel that resembles in many respects the properties of more conventional peptide gels. Therefore, AK16 can be considered as a (first) example of a repulsive gel.

MATERIALS AND METHODS

Materials. For the first series of experiments, Ac-(AAKA)₄-NH₂ (AK16, > 98% purity) was synthesized by Celtek peptides (Nashville, TN) (batch 1). The sample was dialyzed in an aqueous HCl solution for several hours using Spectra/Pore dialysis bags (100–500 Da) in order to remove residual trifluoroacetic acid (TFA). Upon acid exchange, the sample solution was lyophilized for 6 h. For a second series of IR-experiments that were correlated with concomitant rheology measurements, the peptide was obtained from WatsonBio (Houston, Texas) with >98% purity (batch 2). This batch was purchased with a much-reduced TFA content, so that we could skip the dialysis step. Peptide solutions for VCD and FTIR measurements were prepared by dissolving a preweighed amount of purified peptide in D₂O (Sigma-Aldrich). D₂O was used as a solvent to avoid an overlap of the very intense water band at 1640 cm⁻¹ with the vibrational amide I bending modes.²² The homogeneous solution was stored in a conical Eppendorf tube for the duration of the measurements. The final pH of the solution was 2.7 as a result of the dialysis procedure. The pH corresponds to a cation concentration of ca. 2 mM, which lies well below the Cl⁻ concentrations utilized in earlier gelation experiments.²⁰ Moreover, owing to its larger size, unremoved TFA should be significantly less effective than Cl⁻ in shielding the positive lysine charges.

Methods. *FTIR, Vibrational Circular Dichroism (VCD), and Solid State FTIR.* Solid state FTIR spectra were recorded using a Spectrum One FT-IR spectrometer from PerkinElmer (Waltham, MA). A total number of 20 scans were performed with a 4 cm⁻¹ spectral resolution to obtain the IR spectrum. Background subtraction of the solvent spectrum and spectral manipulation were performed using MultiFit.²³ FTIR spectra of liquid samples were recorded using a ChiralIR spectrometer from BioTools (Jupiter, FL). AK16 sample solutions were placed into a 56 μm CaF₂ BioCell (BioTools). Data were collected in 24 h increments, using 8 cm⁻¹ spectral resolution. A total number of 75 scans were performed to obtain the IR spectrum. The run-time to acquire a VCD signal was 360 min. A D₂O IR spectrum was obtained using the same time frame and parameters in order to perform the necessary solvent correction. The instrument was purged with N₂ during the course of the experiment. Background subtraction and spectral manipulation was performed using MultiFit.²³

Atomic Force Microscopy (AFM). AFM images were obtained using a multimode atomic force microscope (Nanoscope IIIa; Digital Instruments, Santa Barbara, CA), equipped with and E-type piezosscanner. The deposited samples were prepared using the same method described above. Fifteen microliters of the 20 mg/mL AK16 hydrogel was deposited onto a freshly cleaned silicon wafer, and allowed to incubate for 15 s. Additionally, 15 μL of D₂O was then used to wash the sample prior to drying under a stream of N₂. Soft tapping mode imaging was performed with a rotated monolithic silicon probe from Budget Sensors (Bulgaria).

Rheology. Frequency sweeps were carried out at 23 °C on a DHR-3 Rheometer (TA Instruments). Samples were loaded between 8 mm plates and surrounded by safflower oil to avoid any solvent evaporation over time. FTIR measurements were recorded in parallel. An amplitude sweep was performed from

0.01 to 1.0% to determine the linear regime for the frequency range of interest: for all measurements, a strain percent of 0.5% was used. Frequency sweeps were conducted from 1.00 to 100 radians/second at room temperature, allowed to hold for 1 min, and then reversed.

RESULTS

For our investigation of AK16 aggregation and gelation we adopted the following protocol. In a first step, we explored the time dependence of the IR-spectra of AK16 in D₂O in the amide I' region for different peptide concentrations between 10 and 20 mg/mL and low ionic strength. The spectra were taken on a daily basis since the results of preliminary experiments had indicated that it might take several days for the sample to gel upon approaching the critical concentration for gelation. The status of the stock solution was checked in parallel to identify any changes of its viscosity. After gelation was obtained, the sample was characterized by AFM. In the third step of our investigation, we combined IR amide I' and rheological measurements in the absence and presence of NaCl to relate specific spectral to the progressing gel formation process.

When discussing the aggregated state of the investigated peptide we will utilize the terminology of Aggeli et al.⁶ Hence, we term an extended β -sheet structure tape; two stacked tapes, a ribbon, and aggregates formed by helically twisted ribbons fibrils. With regard to IR spectroscopy on AK16 we will focus on the amide I' and amide II region of the measured spectra (i.e., 1500–1750 cm⁻¹).

Concentration Dependence of AK16 Aggregation and Gelation. Earlier experiments by Measey et al. have shown that a major fraction of AK16 is preaggregated in β -sheets in the solid state and that these aggregates dissociate rather slowly in water. Therefore, in order to determine the initial state of the AK16 batch (denoted batch 1 in the following) used for our first set of experiments, we measured the FTIR spectrum of solid AK16 between 1400 cm⁻¹ and 1800 cm⁻¹, as shown in Figure S1. The spectrum was decomposed into its minimal set of underlying bands by using the fitting program MULTIFIT.²³ The obtained fitting parameters are listed in Table S1. The satisfactory “goodness of fit” is shown by overlaying the FTIR spectrum as a scatter plot with the solid line obtained from the fitting procedure. Interestingly, we had to use Voigtian profiles for fits to the amide I region above 1600 cm⁻¹, while the spectrum in the region below 1600 cm⁻¹ could be fit as a superposition of Gaussian bands. The amide I region above 1600 cm⁻¹ shows a dominant band at low wavenumbers (1620 cm⁻¹), which is clearly diagnostic of a β -sheet structure with a considerable number of strands.^{24,25} However, the band is unusually broad (total halfwidth of 28 cm⁻¹), which indicates a distribution of different sub-bands with slightly different wavenumber positions. As shown earlier by Lee and Cho as well as by Schweitzer-Stenner,^{24,25} the amide I position shifts to lower wavenumbers with increasing number of strands until saturation is reached for sheets with more than 10 strands. Thus, a distribution of low wavenumber amide I sub-bands can be understood as originating from an inhomogeneous ensemble of rather short β -sheets or alternatively from longer β -sheets that are twisted and/or tilted.²⁶ The sub-band at 1649 cm⁻¹ could be assigned to monomers; the 1675 cm⁻¹ sub-band to trifluoroacetic acid (TFA) present in the purchased batch and the 1695 cm⁻¹ sub-band to the high wavenumber components of typical antiparallel β -sheets and possibly some presence of turn structures in the amorphous solid.²⁷ The ratio of the

integrated intensities of the bands at 1620 and 1649 cm⁻¹ is 2.6, which could indicate that a major fraction of peptides are incorporated in β -sheets. Bands at 1523 and 1557 cm⁻¹ are both assignable to amide II modes of different structures (β -sheets and monomers). Bands below 1500 cm⁻¹ arise from heavily mixed CH₂ and CH₃ deformation modes of side chains.^{28–31} The occurrence of a β -sheet structure in the solid phase does not come as a surprise, since polyalanine or, polypeptides with a high alanine content have a known propensity for this structure in silk protein fibrils.³² The formation of such a regular structure might be facilitated by the deprotonation of the lysine residues in a crystalline/solid environment.

AK16-Disaggregation in D₂O. From earlier results reported by Measey et al. it is clear that any gelation of AK16 in water in the absence of salt requires a peptide concentration above 10 mg/mL and/or a much longer incubation time.²⁰ In a first step, we investigated a sample with a 15 mg/mL protein concentration in D₂O. We measured the IR spectrum of the sample on a daily basis over a period of 4 days after incubation. For each measurement we loaded the BioCell of our IR-spectrometer with a fresh peptide solution. Earlier, preliminary measurements where we had left the sample in the cell over several days had led to rather abnormal results, which we attributed to a drying out of the sample (Sassimovich, Toal, Schweitzer-Stenner, unpublished). Here, we focus on the region between 1500 and 1800 cm⁻¹, which contains the amide II and amide I/amide I' band profiles. The corresponding time dependent spectra are displayed in Figure 1. The intensity of amide II is an indicator of the fraction of the peptide groups for which the amide proton has not been replaced with a deuteron. Its decay over time reflects a very slow NH \leftrightarrow ND exchange.³³ On day 1, the amide I region displays a relatively narrow band at ca. 1616 cm⁻¹, a very broad band at 1645 cm⁻¹, and a weak band at ca. 1690 cm⁻¹. Over a time period of 4 days the intensity of the β -sheet marker band at 1616 cm⁻¹ decreases while the relative intensity of the 1645 cm⁻¹ band increases. We observed an isosbestic point at ca. 1629 cm⁻¹, which indicates a transition between two different states. Apparently, our data indicate a slow decay of the initially present β -sheet tapes or ribbons into either unstructured monomers or amorphous aggregates. This observation and the absence of any observable gelation, or any increase in viscosity after 4 days suggested to us that an extension of the measurement to longer times was unnecessary.

To obtain some more quantitative information from the spectra in Figure 1 we used our program MULTIFIT²³ to decompose the spectrum into Gaussian bands. An example of the spectral decomposition is shown in Figure S2. Again, the satisfactory quality of the fitting is demonstrated by overlaying the FTIR spectrum as a scatter plot with the solid line representing the fit to the spectrum. The obtained spectral parameters are listed in Table S1. We used a minimal number of bands and assumed that only the integrated intensities of the bands changed over time, while the respective band positions and halfwidths were kept constant. This yielded good fits to all spectra in Figure 1. The time dependence of the integrated intensities of the identified amide I' bands (cf. Figure S2) are also exhibited in Figure 1. Figure S3 shows the corresponding time dependence of amide II. The broad and asymmetric band profile of amide I' recorded between 1600 and 1700 cm⁻¹ was decomposed into four sub-bands at 1616, 1632, 1646, and 1690 cm⁻¹, termed AI₁, AI₂, AI₃, and AI₄, respectively. Generally

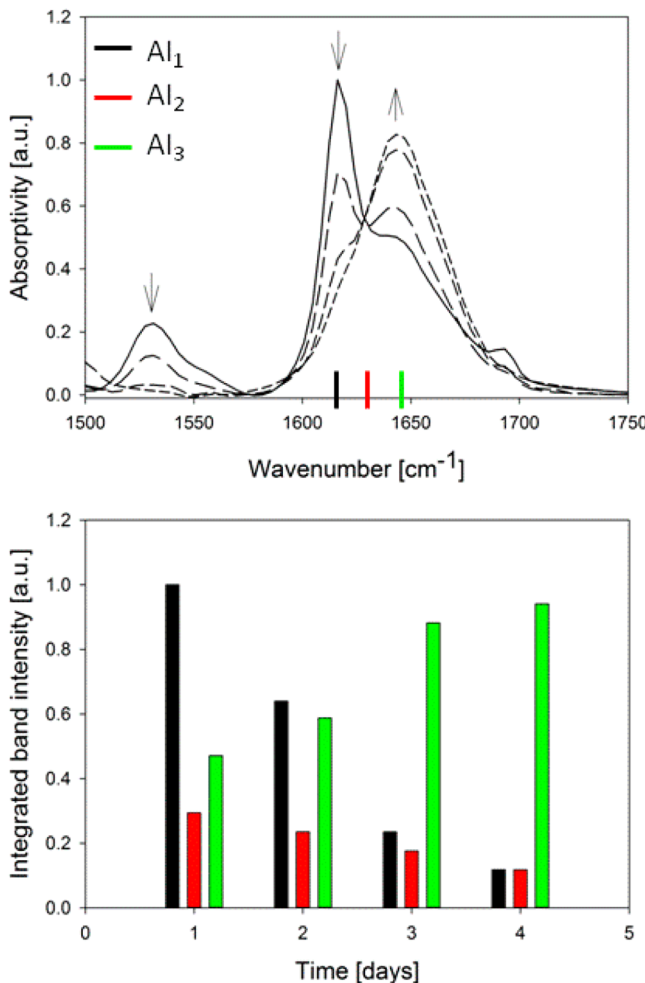


Figure 1. Upper figure: IR spectrum of the amide II and amide I' region of a 15 mg/mL AK16 solution (batch 1) in D₂O recorded between 1500 and 1750 cm⁻¹ over the course of 4 days in 24 h intervals. Spectral changes over time in different spectral regions are indicated by the solid to short dashed lines. The development of the spectrum over time is also indicated by arrows. All spectra were normalized by scaling the peak intensity of the 1616 cm⁻¹ band of the spectrum recorded right after incubation of the peptide (day 1, solid line) to 1. The position of three amide I' sub-bands termed Al₁ (black), Al₂ (red), and Al₃ (green) are indicated. Lower figure: Integrated intensities of Al₁ (1616 cm⁻¹, black), Al₂ (1632 cm⁻¹, red), and Al₃ (1648 cm⁻¹, green) obtained from the spectral decomposition of the amide I' band profiles measured on the indicated days after incubation.

accepted (secondary) structure–amide I wavenumber relations suggest that Al₁ and Al₂ should be attributed to different β -sheet conformations.³⁴ The intense peak at 1616 cm⁻¹ (Al₁) is diagnostic of an extended highly ordered β -sheet with more than 10 strands.²⁵ For heavily tilted or twisted or ordered β -sheets with only a few strands this band is expected to appear at higher wavenumbers.³⁵ Al₂ can therefore be assigned to rather short β -sheet oligomers, such as dimers or trimers or longer tapes with a rather twisted structure (*vide supra*). The peak position of the weak Al₃ band suggests that it should be assignable to a statistical coil with a large polyproline II content.³⁶ The latter assignment based solely on IR data could be problematic, because deviations from an ideal antiparallel β -sheet structure could make otherwise IR-silent amide I' modes IR active.²⁴ However, the anticorrelation between the intensity

increase of Al₃ and the intensity decrease of Al₁ rules out this possibility. The small peak at 1690 cm⁻¹ (Al₄) indicates an antiparallel arrangement, in agreement with Measey et al.²⁰ In what follows we will focus on the sub-bands Al₁–Al₃. Another band that appears around 1675 cm⁻¹ is assigned to residual TFA not removed during purification. These spectroscopic data clearly show that in an initial phase AK16 maintains its highly ordered β -sheet structure even after its dissolution in water, where it decays over a period of several days. Our data (Figure 1) suggest that only 10% of the original β -sheet fraction was left after 4 days. Interestingly, the amide II intensity decreases a little bit faster than Al₁ (Figures S3 and 1), suggesting that the fragmentation of aggregates facilitates the accessibility of backbone groups to the solvent.

We characterize the obtained intensity changes further by defining the enhancement parameter:

$$r = \frac{I_{A_{1,\infty}} + I_{A_{2,\infty}}}{I_{A_{1,0}} + I_{A_{2,0}} - (I_{A_{3,\infty}} - I_{A_{3,0}})} \quad (1)$$

where I₀ and I _{∞} values are respective intensities measured on day 1 and day 4, respectively. If $r < 1/r > 1$, the decrease/increase of the total amide I intensity assignable to β -sheet structures ($I_{A_1}+I_{A_2}$) is not fully accounted for by the increase/decrease of Al₃. An r-value of 1 would indicate that the observed intensity change of the amide I' intensity distribution is solely due to the conformational redistribution. From the respective parameters obtained from the fits to the data in Figure 1 we derived an r-value of 0.25, which indicates a loss of oscillator strength during the disaggregation process.

The above experimental data clearly suggest that a peptide concentration of 15 mg/mL is insufficient for maintaining the aggregation state of the peptide over the time and therefore also insufficient for gelation. This result seems to be somewhat at variance with the rather stationary β -sheet aggregation state of 10 mg/mL AK16 reported by Measey et al.²⁰ However, their data covered only a time period of 150 min. In order to relate ours with their data, we prepared a 10 mg/mL AK16 sample and measured the time dependence of its IR spectrum. Figure S4 shows the 1500–1750 cm⁻¹ region of the spectrum measured over a time period of 5 days. The observed spectral changes were minimal. All spectra were decomposed into the same bands used for the spectral analysis of the 15 mg/mL sample. The corresponding relative intensities of Al₁ (1616 cm⁻¹), Al₂ (1632 cm⁻¹), and Al₃ (1648 cm⁻¹) are displayed in Figure S5. Apparently, even in the day 1 spectrum the intensities of the β -sheet markers Al₁ and Al₂ are very weak; the amide I region is thus dominated by Al₃ which indicates that most of the initially existing peptide aggregates did dissociate before the first measurement was made. Taken together, the 10 and 15 mg/mL data clearly suggest that the rate of the decay of the initially present β -sheets decreases with increasing peptide concentration, in qualitative agreement with Measey et al.²⁰

The next step in our attempt to identify the conditions required for AK16 gelation in the absence of NaCl involved the daily measurement of the IR spectrum of 20 mg/mL AK16 sample over a period of five consecutive days. The termination of the measurements after 5 days was prompted by the visible gelation of the sample. The 1500–1750 cm⁻¹ region of the respective spectra are shown in Figure 2. The observed changes in all spectral regions differ very much from what we have observed for the 15 mg/mL sample. Even in the spectrum measured right after incubation, the Al₁ band appears at a

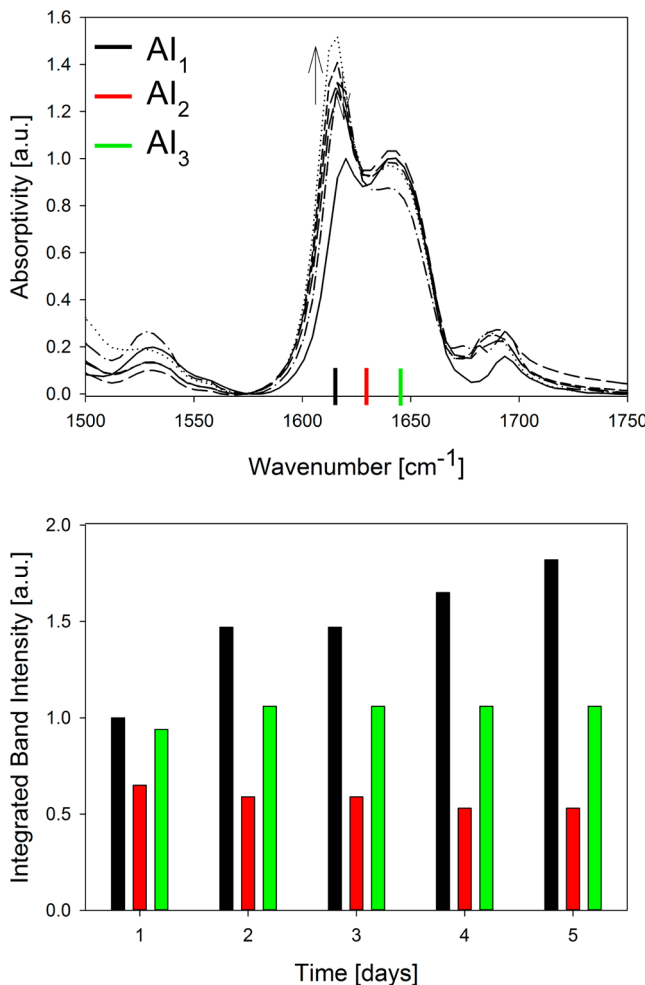


Figure 2. Upper figure: IR spectrum of the amide II and amide I' region of a 20 mg/mL AK16 solution (batch 1) in D₂O recorded between 1500 and 1750 cm⁻¹ over the course of 4 days in 24 h intervals. Spectral changes over time in different spectral regions are indicated by the solid to short dashed lines. The development of the spectrum over time is also indicated by arrows. All spectra were normalized by scaling the peak intensity of the 1616 cm⁻¹ band of the spectrum recorded right after incubation of the peptide (day 1, solid line) to 1. The position of three amide I' sub-bands termed AI₁ (black), AI₂ (red), and AI₃ (green) are indicated. Lower figure: Integrated intensities of AI₁ (1616 cm⁻¹, black), AI₂ (1632 cm⁻¹, red), and AI₃ (1648 cm⁻¹, green) obtained from the spectral decomposition of the amide I' band profiles measured on the indicated days after incubation.

slightly downshifted position of 1612 cm⁻¹. Its integrated intensity now significantly increases over time (Figure 2). This increase is not correlated with a corresponding decrease of the total intensity of the remaining amide I' sub-bands that are now positioned at 1636 cm⁻¹ (AI₂) and 1648 cm⁻¹ (AI₃). The intensity of AI₂ decays only slightly and a substantial intensity remains at the end of the investigated time period. The AI₃-band actually increases its intensity. These observations suggest that the observed intensity increase, particularly of AI₁, must be related to changes of the mode's oscillator strength and does not reflect redistribution within the conformational ensemble of the peptide. The increase of the AI₁ intensity involves two phases (Figure 2). The first one is completed after 2 days; the second, less pronounced phase, occurs between day 3 and 5. An *r*-value of 1.52, which we obtained by using intensity values

measured on day 1 and 5 for I_0 and I_∞ , respectively, reflects the disproportional enhancement of AI₁. Our results suggests that AK16 can indeed form a hydrogel even in the absence of supporting anions if the concentration is high enough so that the gelation process becomes faster than the $\beta \rightarrow$ disordered state decay of the peptide. Moreover, the increase and slight downshift of AI₁ could be considered as an indicator of a β -sheet structure in cross-linked fibrils that form the network required for hydrogel formation.

Initial and final states of 20 mg/mL AK16 in D₂O are further characterized by VCD spectroscopy (Figure S6). In the spectrum measured at day 1, the amide I' region solely displays a negative triplet at the position of the AI₃ band. The amplitude of the signal strongly suggests a disordered state dominated by the sampling of pII conformations by the individual amino acid residues,³⁷ which corroborates the above assignment of the AI₃-band further. There is no signal at the position of the two β -sheet bands, which suggests rather ideal antisymmetric β -sheets without any noteworthy helical twist.³⁸ A very weak negative Cotton band seems to exist at the amide II position. The second spectrum in Figure S6, which was taken after gelation, exhibits a negative triplet with a slight positive bias at the AI₂ position, which is overlaid by a negative signal coinciding with the dominant AI₁ band. The positive bias of the pII signal suggests that its negative component overlaps with the positive part of the signal associated with AI₁ band. The occurrence of rotational strength at this position can have two sources: the observed increase in modes' oscillator strength (intrinsic intensity) and/or a helical twist of the β -sheet tape,³⁸ which according to Aggeli et al. is a prerequisite of gel formation.⁶

We also investigated the formed hydrogel with AFM. The corresponding image shown in Figure 3 (upper panel) shows a morphology similar to that of the complex nanoweb observed by Measey et al. for salt induced gels of AK16 and reported in several studies for hydrogels formed by zwitterionic peptides.²⁰ This suggests a gel of comparable stability. We also obtained an AFM image for AK16 in the solution state, as a point of comparison (Figure 3, lower figure). It shows a mixture of small scale (40–80 nm) and rather large-scale aggregates with a branched, fractal structure, which is clearly distinct from the dense nanoweb of comparatively thin fibrils displayed in the image of the gel state.

The data shown thus far suggest the following scenario of AK16 aggregation in gelation. A fraction of the peptide is preaggregated in β -sheet like structures, which decay very slowly in aqueous solution. The higher the peptide concentration the slower is this disaggregation process. Above a certain critical concentration which lies somewhere between 15 and 20 mg/mL, the peptide β -sheet structures become so stable that the conditions in the sample become permissible for further cross-linking and eventually gelation. The spectral changes in the amide I' band region of the 20 mg/mL sample suggest a rearrangement of the β -sheet structures which eventually facilitates gelation. This view is consistent with the rather different AFM images of aggregates in solution and in the gel phase.

We wondered whether we could narrow down the critical concentration by incubating 17.5 mg/mL of the peptide in D₂O and wait for its gelation. We found that it did so after 60 days. IR spectra taken on day 1, day 30, and the day of gelation are shown in Figure S7. Compared with what we observed for the 15 mg/mL and the 20 mg/mL sample the observed spectral

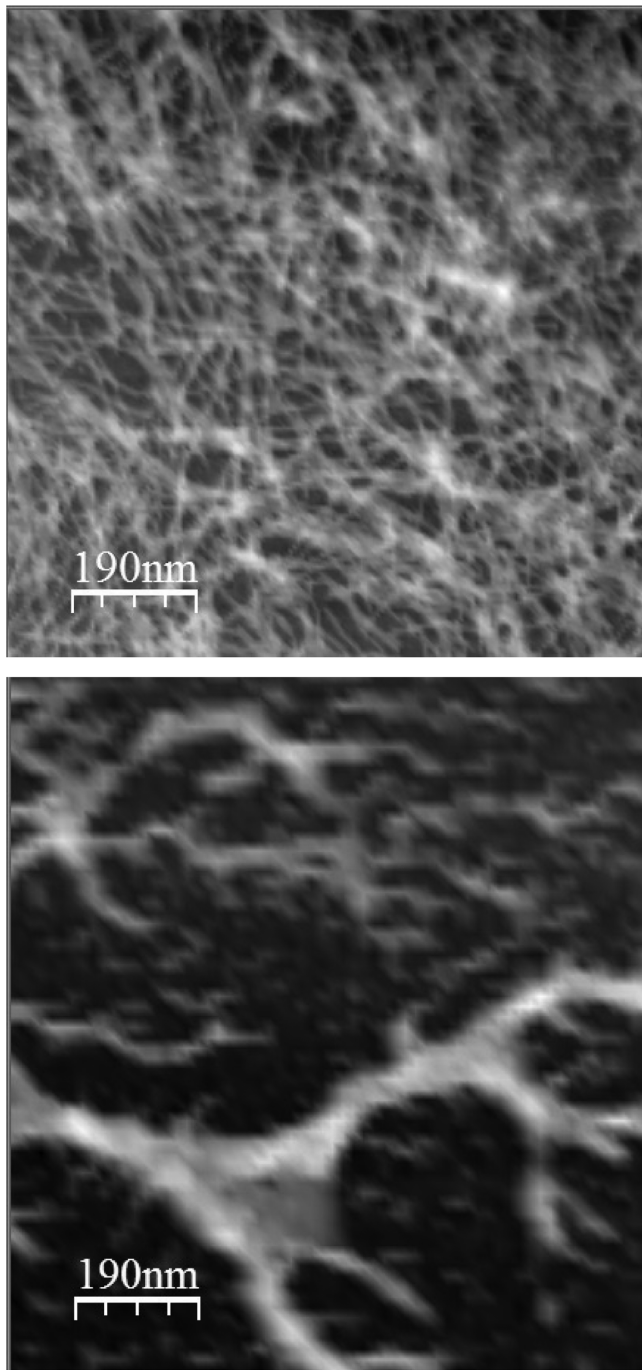


Figure 3. AFM height images of 20 mg/mL AK16 (batch 1) after gel formation (upper panel) and a 8 mg/mL AK16 (lower panel) right after incubation deposited onto a silicon surface.

changes are minimal. Overall, we estimate an r factor of 1.2 from the data, which indicate a modest increase of the AI' oscillator strength. These data suggest that the critical concentration for the AK16 gelation at low ionic strength lies only slightly above 17.5 mg/mL.

Combining IR and Rheology. In order to probe the formation of the gel phase more directly, we prepared a second stock solution of 20 mg/mL AK16 in D₂O from the newly purchased batch of peptides (termed batch 2 in the following), and performed IR and rheological measurements in tandem. The spectral decomposition of the IR-spectrum of the solid sample in Figure S8 yielded an AI₁/AI₂ intensity ratio of 1.04,

which suggests that compared with the batch used for the above-described experiments a significantly lesser fraction of peptides is incorporated in β -sheet like structures. The wavenumbers and integrated intensities of the obtained bands are listed in Table S2.

Figure 4 shows the overlaid FTIR spectra of the new 20 mg/mL AK16 sample as recorded daily over a period of 5 days. A

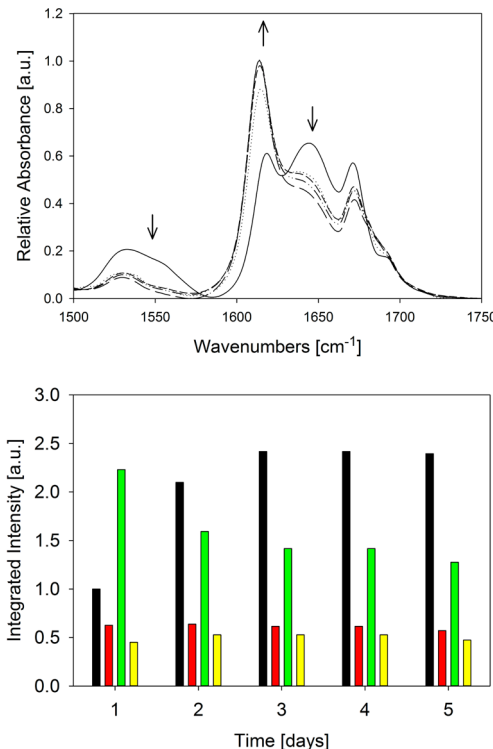


Figure 4. Upper figure: IR spectrum of the amide II and amide I' region of 20 mg/mL AK16 (batch 2) in D₂O measured between 1580 and 1800 cm⁻¹ over the course of 4 days in 24 h intervals in tangent with rheological data. Spectral changes over time are marked by arrows. Lower figure: Integrated intensities of AI₁ (black), AI₂ (red), and AI₃ (green) obtained from the spectral decomposition of the amide I' band profiles measured on the indicated days after incubation. The yellow bars indicate the intensity of the TFA band, which has not been removed from the spectrum in order to serve as a reference for the intensity variations of the amide I' sub-bands.

spectral decomposition using the above introduced spectral model for the amide I' region yielded the time dependence of individual amide I' sub-bands depicted in Figure 4. Four observations are noteworthy. First, AI₁ is initially much less and AI₃ is more intense than the corresponding bands in the spectrum of the above investigated 20 mg/mL sample (Figure 2). The intensity ratio $I(\text{AI}_1)/I(\text{AI}_3)$ is 0.45, which suggests that right after incubation the sample contained less peptides incorporated in β -sheets and a higher percentage of peptides with statistical coil like structures than the corresponding sample used for the first series of spectroscopic measurements (*vide supra*). This observation is consistent with what we observed for the respective solid samples of the two batches. Second, the increase of AI₁ over time and the subsequent decrease of AI₃ reflect the reformation of β -sheet structures. The intensities of both bands level off after the third day. Concomitantly, we observed a small downshift of AI₁ (from 1616 to 1613 cm⁻¹), thus reproducing a similar observation

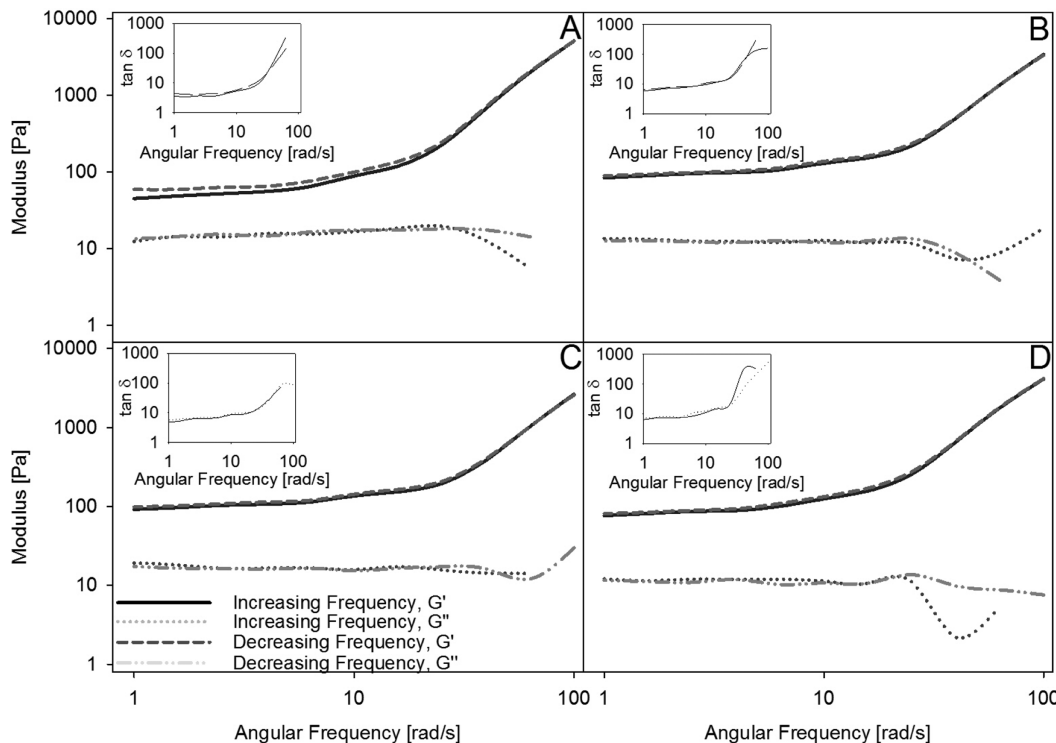


Figure 5. Rheological frequency sweeps of storage, G' , and loss, G'' , moduli at 23 °C for the 20 mg/mL AK16 sample (batch 2) (A) immediately after preparation, as well as after an incubation time of (B) 48 h, (C) 72 h, and (D) 96 h. Each cycle of the sweep involved increasing the angular frequency, stabilizing for 1 min, and then decreasing the angular frequency. Ten sweeps were taken in total and the average is shown here.

made for the first 20 mg/L sample (*vide supra*). Third, the r -value estimated from the observed AI_1 and AI_3 values is 1.23 thus indicating a less pronounced increase of the β -sheet related amide I oscillator strength (AI_1 and AI_2) compared with what we observed for the first sample. Fourth, gelation was evidenced by a very viscous sample on the third day of our experiment.

To characterize the rheological properties of the sample, we performed frequency sweeps to determine the storage modulus, G' , as well as the loss modulus, G'' , as a function of frequency. Figure 5 shows the frequency sweeps for G' and G'' of 20 mg/mL AK16 in D_2O over the course of 4 days. Even on day 1, $G' > G''$, indicating the formation of a solid gel, which is viscoelastic at low frequency and more solid-like at high frequency, where the loss factor $\tan \delta$ becomes very large. G' increases from 88 to 147 Pa at 10 s^{-1} from day 1 to day 3 and is unchanged on day 4. The G' and $\tan \delta$ values are quantitatively similar to that reported for more conventional peptide hydrogels, such as RATEA16,¹⁰ hydrophobic short peptide gels,³⁹ and the glutamine rich peptides of Aggeli et al.,⁶ but is less rigid than the gel formed by the β -hairpin-type fibrils of the MAX1 peptides reported by Schneider et al.⁴⁰ The observed increase of G' over time coincides with the above-described increase of AI_1 (and in part A_2), which suggests a correlation between the increase of the AI_1 oscillation strength and the increasing strength of the gel phase that result from further cross-linking to form the above nanoweb structure.

The results of the studies on the second 20 mg/mL sample of AK16 suggest that gelation starts much earlier than indicated by the visible change of a sample's viscosity. It is therefore likely that the spectral changes observed for the first 20 mg/mL sample shown in Figure 2 and 4 are all gelation-related even though the sample inspection revealed gelation only 5 days after incubation. The extent of AI_1 enhancement might depend

on the individual sample conditions of the aggregation and gelation process, which is clearly different for the two investigated 20 mg/mL samples.

The comparatively fast gelation of the second 20 mg/mL sample suggests that the preceding dissociation of the initial aggregates into either monomers or amorphous aggregates actually facilitates gelation by allowing newly formed β -sheet fibrils to form the nanoweb structure shown in Figure 3. In order to check the validity of this supposition we produced another 20 mg/mL sample of AK16 with peptides from batch 2 and subjected it to sonication. The IR spectra of the sample measured right after sonication (solid line) and 5 h later (dashed line) are shown in Figure 6. Both spectra are very similar and indicative of a sample that is dominated by β -sheet like structures. Only the AI_1 band increased slightly during the 5 h period. The sample was found to gel immediately. To further characterize the gel phase, rheological measurements were carried out on the sample after the 5 h incubation period. As shown in Figure 7 the storage modulus is similar in magnitude to that of the unsonicated 20 mg/mL sample after it had gelled (*vide supra*, Figure 5). These results suggest that the disruption of the initial β -sheet aggregates actually accelerated the reaggregation and gelation considerably by providing a higher concentration of fragments, which served as a nucleation site for β -sheet formation and gelation.

Taken together, all the observation made with 20 mg/mL AK16 samples strongly corroborated the notion that AK16 can form hydrogels even in the absence of a sufficient amount of neutralizing anions.

Hydrogelation in the Presence of Salt. As shown by Measey et al.²⁰ AK16 forms a hydrogel instantaneously upon addition of salts for peptide concentrations above 5 mg/mL. This has been attributed to a shielding of the positive charges

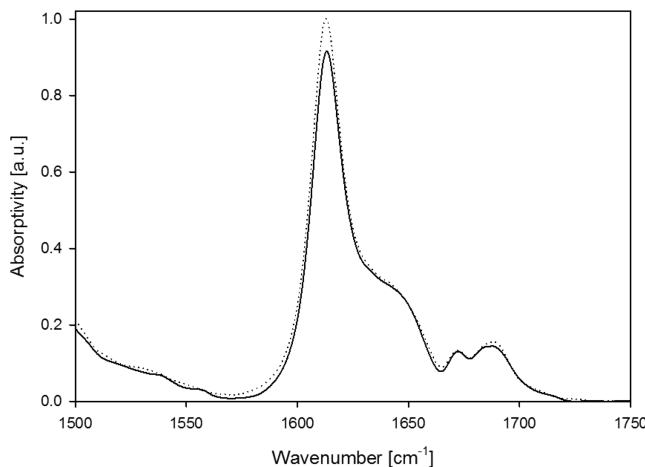


Figure 6. IR spectrum of the amide II and amide I' region of 20 mg/mL AK16 in D_2O measured between 1500 and 1750 cm^{-1} directly following (solid line) and 4 h after (dashed line) sonication.

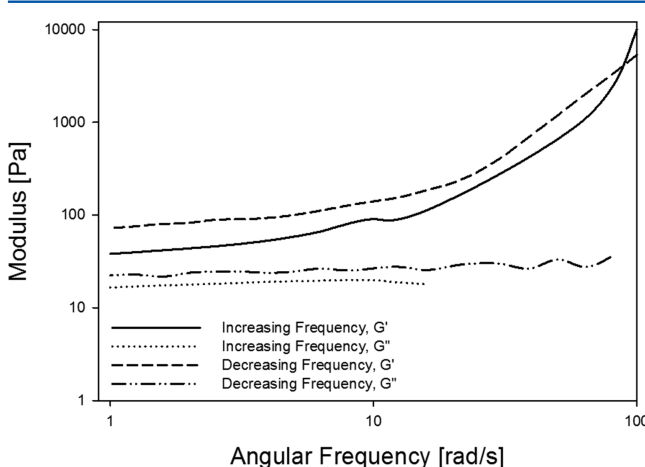


Figure 7. Rheological frequency sweeps of storage, G' , and loss, G'' , moduli at 23 $^{\circ}\text{C}$ for the 20 mg/mL AK16 sample 4 h after sonication. Each cycle of the sweep involved increasing the angular frequency, stabilizing for 1 min, and then decreasing the angular frequency. Ten sweeps were taken in total and the average is shown here.

on the lysine residues by electrostatic screening. The question arises whether AK16 hydrogels formed in the presence and absence of salt are comparable in both rheological and spectroscopic terms. Figure 8 shows the amide I spectrum of AK16 at a concentration of 5 mg/mL recorded prior to the addition of NaCl, and subsequently 30 and 60 min after adding 1.2 M NaCl. We chose this relatively low concentration of the peptide to allow for a comparison with corresponding data of Measey et al. and to avoid gel formation prior to the addition of salt. The spectrum measured in the absence of salt indicates only a minor population of β -sheet ($I(\text{AI}_1)/I(\text{AI}_3) = 0.14$). The addition of NaCl leads to a comparatively rapid increase of the AI_1 band, which indicates conversion of statistical coil peptides into β -sheets. We decomposed the spectra into their underlying bands (*vide supra*) and plotted the intensities as a function of time in Figure 8. From the obtained data we estimated an r factor of 1.8, which is even larger than the value obtained for the first gel-forming batch in the absence of NaCl (1.55, *vide supra*). As demonstrated by the rheology data exhibited in Figure 9, the addition of NaCl caused a gelation of the sample. Figure 9a depicts the G' and G'' spectrum of the peptide in the

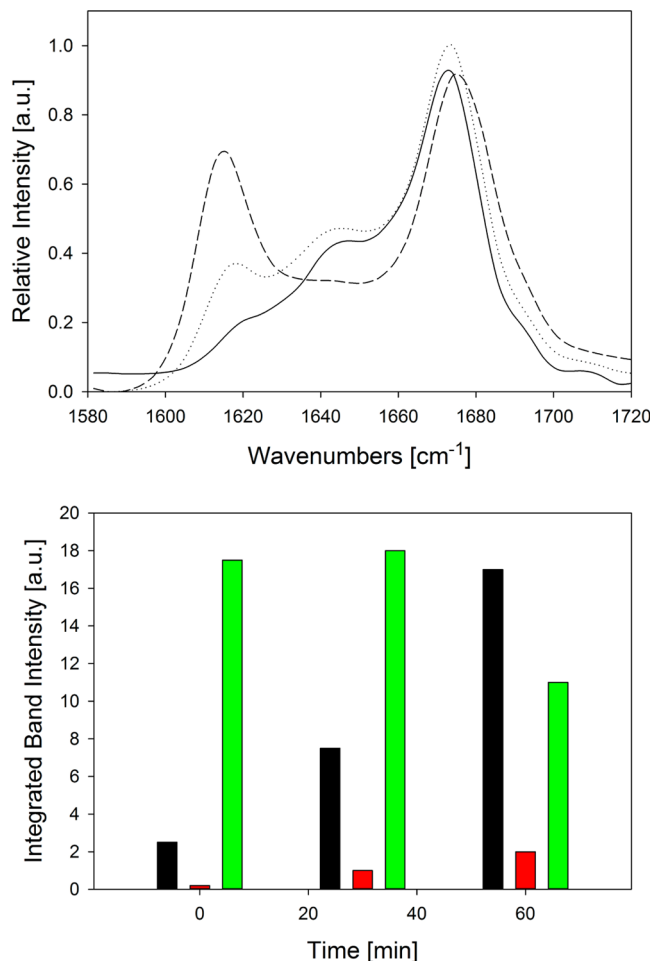


Figure 8. Upper figure: IR spectrum of the amide II and amide I' region of 5 mg/mL AK16 in D_2O (batch 2) measured between 1580 and 1720 cm^{-1} without salt and then 30 and 60 min after the addition of 1.2 M NaCl. The development of the spectrum over time is indicated by arrows. Lower figure: Integrated intensities of AI_1 (black), AI_2 (red), and AI_3 (green) obtained from the spectral decomposition of the amide I' band profiles measured on the indicated time (at the corresponding red bar) after incubation.

absence of salt after a 96 h incubation (replotted data from Figure 6), while Figure 9b shows the respective spectra of the peptide in the presence of salt after an incubation time of 1 h. They both show similar characteristics with the trend of the storage and loss moduli, i.e., a viscoelastic solid at low frequency and an increasingly stronger solid at high frequencies. The similarity both qualitatively and quantitatively, between the rheological responses and the spectroscopic properties of the two-peptide solutions, clearly indicates that screening charges have no effect on the final structure and the strength of the gel. Therefore, we can conclude that NaCl solely serves as a catalyst of the gelation process, which significantly increases the rate of gelation.

DISCUSSION

Summary of Results. The results of our investigation of AK16-aggregation in the absence of a sufficient amount of charge-shielding anions unambiguously show that this cationic peptide with a charge surplus of +4 can form a hydrogel. The time scale of the gelation process seems to increase with decreasing initial concentration of β -sheet tapes/ribbons which

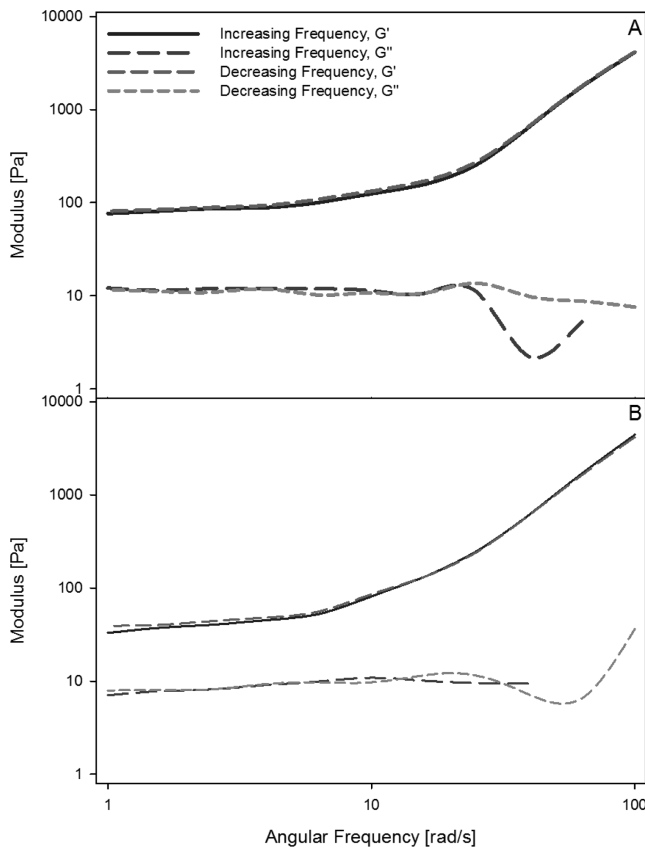
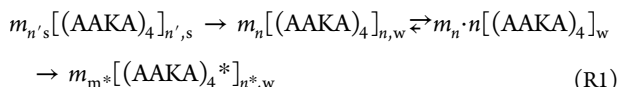


Figure 9. Rheological frequency sweeps of storage, G' , and loss, G'' , moduli at 23 °C of (a) 20 mg/mL AK16 after 96 h and (b) 5 mg/mL AK16 with 1.2 M NaCl in D_2O of a fully formed hydrogels.

suggests that gelation requires the reaggregation of peptides into fibrillar structures which are than capable of building the nanoweb-like network required for the immobilization of water molecules. This view is strongly supported by the AFM images of the solution and the gel phase of AK16. An elimination of preformed aggregates by sonication accelerates the gelation process dramatically. The addition of an excess of NaCl led to rather quick reaggregation and gelation of the 5 mg/mL AK16. The formed gel showed G' and G'' values comparable to those of the gel obtained without adding salt. Taken together, our data reveal that in spite of its highly cationic character AK16 can self-aggregate and gelate and that the addition of NaCl just reduces the activation energy of the aggregation process.

Kinetics and Concentration Dependence of AK16 Aggregation. The kinetics of AK16 formation and its dependence on peptide concentration is rather peculiar. Generally, the process of self-aggregation is preceded by a nucleation phase, which involves the formation of short oligomers and amorphous aggregates.³ Subsequently, peptides undergo disorder → order phase transitions that are highly cooperative. The data thus far obtained for AK16 in aqueous solution suggest a different picture, which can be represented by the following reaction scheme:



where $m_{j,s/w}$ denotes the number of tapes with $j = 1, 2, 3, \dots, p, \dots, n$ (n, n^*) AK16 strands in the solid (s) and the aqueous (w) environment. The first process involves the dissolution of the

preaggregated peptides that leads to the (partial) solvation of the β -sheets and thus to the observed downshift of A_1 . This step is followed by the dissociation of these extended β -sheet structures and the formation of amorphous aggregates, which constitute the nucleation phase for the third reaction, i.e., the formation of a nanoweb network of amyloid like fibrils which causes the sample to gel. Below a critical concentration which lies somewhere between 15 and 17 mg/mL, the reformation of β -sheet tapes and fibrils is not initiated on the time scale of our experiment.⁴¹ Above this critical concentration, AK16 reaggregates and concomitantly gels. If the time scales of the dissociation and the reaggregation processes overlap, the still present β -sheets can accelerate the reaggregation by promoting secondary nucleation. The rheological data suggest the gelation developed practically in sync with fibril formation. In the presence of NaCl gelation is accelerated owing to the shielding of positively charged peptides by Cl⁻ anions. Subjecting the sample to sonication right after incubation might produce shorter fragments, which efficiently catalyze reaggregation and thus gelation.

AFM Data. Figure 10a exhibits a height histogram of the AFM image of the 20 mg/mL sample shown in Figure 3. The

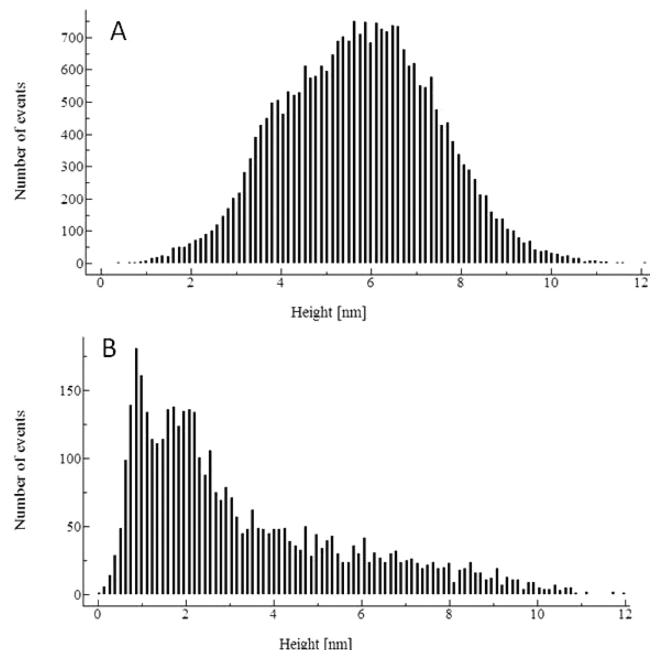


Figure 10. Height histogram obtained from the AFM height images of 20 mg/mL (upper panel) and 8 mg/mL AK16 (lower panel).

distribution is rather broad and indicates a superposition of two Gaussian like distributions with maxima at 4.0 and 6.8 nm. The situation is different for the AFM image of an 8 mg/mL sample for which the height profile indicates two maxima at 1 and 2 nm (Figure 10b). However, the profile is highly asymmetric and contribution in the region between 3 and 10 nm are noteworthy. The average heights for two different peptides concentrations (8 and 20 mg/mL) are 3 and 6 nm, respectively. If one assumes an average distance of 1 nm between sheets in tapes comprised of two sheets/tapes,⁴² our data suggest rather thick fibrils, which are formed by stacking between 2 and 6 strands. While the formation of a tape with two strands is easily imaginable as a result of strong hydrophobic interactions between the aliphatic alanine containing side of β -sheets,¹⁷

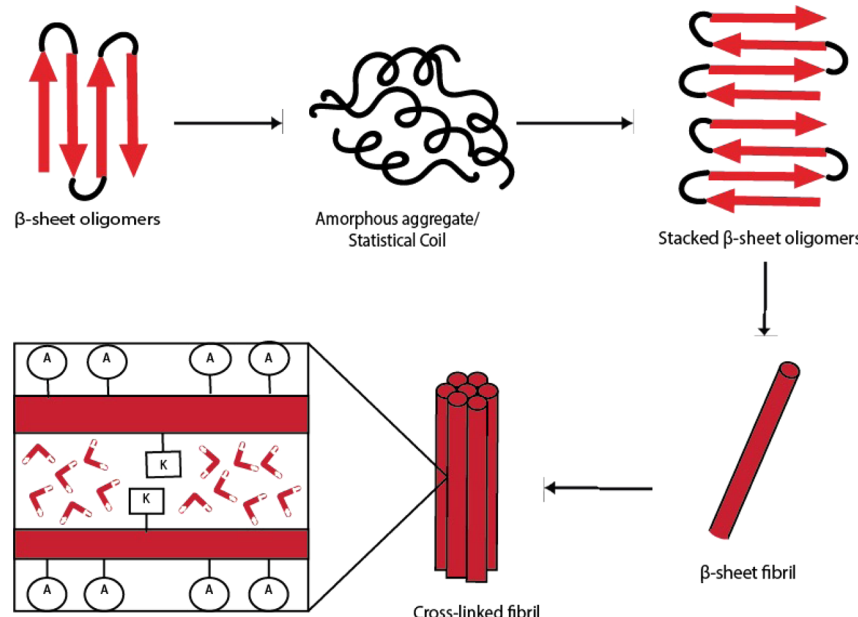


Figure 11. Schematic representation of the proposed mechanism of gelation of AK16 in water. The upper part of the figure illustrates the transitions between the initial and final β -sheet fibrils via an intermediate state of amorphous aggregates. The lower part visualizes the proposed stacking of β -sheets in hydrogels, which exhibit alternate hydrophobic and aqueous/hydrophilic interfaces.

further stacking would be impeded by the repulsive interactions between the lysine side chains of the hydrophilic sides. As a possible solution we propose a double-layer structure (Figure 11) with alternating hydrophobic (alanine) and (immobilized) water interfaces (by lysine residues). Each strand of the double layer represents an extended β -sheet tape. In other words we suggest a network of hydrogen bonded water molecules that connect the ammonium groups of the protonated lysine residues and might also involve peptide carbonyl groups which can accept another hydrogen bond in addition to the canonical interpeptide hydrogen bonding between strands in β -sheet structures. Such a network could be strengthened by the involvement of the still existing Cl^- ions, which can complex with NH-groups of the peptide and the lysine side chain as well as with the HO-group of water molecules.⁴³

Aggregation and Amide I Intensity. Why does β -sheet aggregation cause the significant increase of the amide I oscillator strength, which reflects significant changes of the normal mode composition or of the charge distribution of the peptide group? Significant changes of the amide I oscillator strength have been observed and discussed before. Manas et al. investigated the amide I' of *N*-methylacetamide (NMA) and of isotopically labeled residues of the helical protein termed GCN4-PI' in 50% D_2O /50% glycerol mixtures.⁴⁴ They found slight downshifts and rather significant increases of the amide I' of hydrated peptide groups with decreasing temperature. At 170 K the solvent switches from a liquid to a glass-like state. Below this temperature all spectral parameters become temperature independent. The downshifts of the amide I' bands between room and glass transition temperature are comparable with what we observe in our experiment for the dominant AI_1 band (*vide supra*) upon gelation. The concomitant change of the amide I' intensity of NMA indicates an increase of the oscillator strength by a factor of 1.4. The respective intensity changes of the amide I' contribution of isotopically labeled GCN4-PI' peptide groups exhibit an even larger increase (1.6). Both values are close to what we observed

for the AI_1 intensity increase of batch 1 of 20 mg/mL AK16 (~1.5), and for the corresponding AI_1 increase of 5 mg/mL AK16 in the presence of NaCl (~1.7).

Computational studies clearly demonstrate that both, the wavenumber and to a larger extent the oscillator strength of amide I/amide I' depend on the electrostatic properties of the solute, on peptide-solvent hydrogen bonding and on the size of the cavity that the solvent forms around the solute.⁴⁵ In line with how Manas et al. explained the amide I' temperature dependence of NMA and GCN4-PI', we tentatively propose that the amide I' intensity increase observed in this study reflects increasing water immobilization which can occur in the rather thick fractal aggregates shown in Figure 9a and in the nanoweb structure displayed in Figure 9b.

We envision two modes of interaction that could lead to water immobilization. First, we invoke the results of a recent computational study on the hydration of an antiparallel β -sheet, which suggest that water molecules predominantly occupy various grooves formed in this type of secondary structure.⁴⁶ At least part of these water molecules can still donate hydrogen bonds to the C=O bonds of peptide groups. Upon ribbon formation (sheet stacking) of AK16 these water molecules would get caught in a rather hydrophobic environment formed by the alanine residues on the aliphatic side of the interacting tapes (β -sheets). Additional immobilization of water could involve the lysine residues on the hydrophilic side of ribbons (fibrils). One can expect the ammonium groups of lysines to be heavily hydrated. In the nanoweb structure, water gets sequestered in cells the sizes of which cover a rather broad range on the 10–150 nm scale. It is well thinkable that the lysine residues assist in immobilizing water in these cells the same way as hydrophilic groups do so with water captured in reversed micelles.⁴⁷ The addition of NaCl could support the water immobilization in these cells further.

SUMMARY

Here, we studied the time dependence of aggregation and subsequent hydrogelation of the strongly cationic peptide, AK16 at low ionic strength. The behavior of AK16 at low and high concentrations was studied by probing the amide I' band in the infrared spectrum. The amide I' band was heuristically decomposed for each 24 h time marker into its respective sub-bands, AI₁, AI₂, and AI₃. Each sub-band is a marker for secondary structure, and was monitored as a function of time. We first examined the behavior of soluble aggregates at 15 mg/mL. The peptide at this lower concentration shows behavior similar to an inverse nucleation phase, where pre-existing unstable β -sheets decay into a disordered ensemble. At a concentration of 20 mg/mL, the sample gelled and incurred major changes of its spectroscopic properties. Rheological data suggest that the formation of a nanoweb of β -sheet fibrils continuously stabilizes the gel. This process is probed by an increase of the intensity of the amide I' band, which cannot be explained in terms of intensity redistribution caused by conformational changes. We propose a mechanism wherein the initial β -sheets decay into a disordered ensemble (much like the peptide at low concentration), which is then used as a nucleation phase for fibrillation. From the information obtained from the AFM images we infer the formation of rather thick fibrils in the gel phase, which must be composed of several layers of stacked β -sheet tapes. As an explanation for this observation, we suggest two possible scenarios, i.e., alternating alanine-lysine (water) and pure alanine (hydrophobic) interfaces within the local structure of the gel. Our data clearly suggest that in the case of AK16 electrostatic repulsion decelerates rather than inhibits aggregation and gelation, contrary to expectation.¹⁶

ASSOCIATED CONTENT

Supporting Information

The Supporting Information is available free of charge on the ACS Publications website at DOI: [10.1021/acs.jpcb.6b07673](https://doi.org/10.1021/acs.jpcb.6b07673).

Tables of spectral decomposition half-widths, FTIR spectra of solid AK-16 from first and second batches, IR spectrum of 10 and 17.5 mg/mL over time, decomposition of 15 mg/mL AK-16 in D₂O, and figures depicting the integrated intensities over time obtained from the FTIR spectra ([PDF](#))

AUTHOR INFORMATION

Corresponding Author

*Telephone: 215-895-2268; E-mail: rschweitzer-stenner@drexel.edu.

Present Address

¹Department of Chemistry and Biochemistry, University of Delaware, Newark, DE 19716

Notes

The authors declare no competing financial interest.

ACKNOWLEDGMENTS

We would like to thank the Chemistry Department at Drexel University for partly funding this work.

REFERENCES

- Kresheck, G. C.; Schneider, H.; Scheraga, H. A. The Effect of D₂O on the Thermal Stability of Proteins. *Thermodynamic Parameters for the Transfer of Model Compounds from H₂O to D₂O. J. Phys. Chem.* **1965**, *69*, 3132–3144.
- Rajagopal, K.; Schneider, J. P. Self-Assembling Peptides and Proteins for Nanotechnological Applications. *Curr. Opin. Struct. Biol.* **2004**, *14*, 480–486.
- Dobson, C. M. Protein Misfolding, Evolution and Disease. *Trends Biochem. Sci.* **1999**, *24*, 329–332.
- Holmes, T. C. Novel Peptide-based Biomaterial Scaffolds for Tissue Engineering. *Trends Biotechnol.* **2002**, *20* (1), 16–21.
- Peppas, N. A.; Huang, Y.-S.; Torres-Lugo, M.; Ward, J. H.; Zhang, J. Physicochemical Foundations and Structural Design of Hydrogels in Medicine and Biology. *Annu. Rev. Biomed. Eng.* **2000**, *2*, 9–29.
- Aggeli, A.; Nyirkova, I. A.; Bell, M.; Harding, R.; Carrick, L.; McLeish, T. C. B.; Semenov, A. N.; Boden, N. Hierarchical Self-Assembly of Chiral Rod-like Molecules as a Model for Peptide β -sheet Tapes, Ribbons, Fibrils and Fibers. *Proc. Natl. Acad. Sci. U. S. A.* **2001**, *98*, 11857–11862.
- Uversky, V. N.; Oldfield, C. J.; Dunker, K. A. Showing your ID: Intrinsic Disorder as an IDP for Recognition, Regulation and Cell Signalling. *J. Mol. Recognit.* **2005**, *18*, 343–384.
- Yokoi, H.; Kinoshita, T. Strategy for Designing Self-Assembling Peptides to Prepare Transparent Nanofiber Hydrogel at Neutral pH. *J. Nanomater.* **2012**, *2012*, 1.
- Yokoi, H.; Kinoshita, T.; Zhang, S. G. Dynamic Reassembly of Peptide RADA16 Nanofiber Scaffold. *Proc. Natl. Acad. Sci. U. S. A.* **2005**, *102* (24), 8414–8419.
- Zhao, Y.; Yokoi, H.; Tanaka, M.; Kinoshita, T.; Tan, T. W. Self-assembled pH-Responsive Hydrogels Composed of the RATEA16 Peptide. *Biomacromolecules* **2008**, *9* (6), 1511–1518.
- Zou, D.; Tie, Z.; Lu, C.; Qin, M.; Lu, X.; Wang, M.; Wang, W.; Chen, P. Effects of Hydrophobicity and Anions on Self-Assembly of the Peptide EMK 16-II. *Biopolymers* **2009**, *93*, 318–329.
- Caplan, M. R.; Schwartzbarf, E. M.; Zhang, S.; Kamm, R. D.; Lauffenburger, D. A. Control of Self-assembling Oligopeptide Matrix Formation through Systematic Variation of Amino Acid Sequence. *Biomaterials* **2002**, *23*, 219–227.
- De Leon Rodriguez, L. M.; Hemar, Y.; Cornish, J.; Brimble, M. A. Structure-mechanical Property Correlations of Hydrogel forming Beta-Sheet Peptides. *Chem. Soc. Rev.* **2016**, *45*, 4797–4824.
- Caplan, M. R.; Moore, P. N.; Zhang, S.; Kamm, R. D.; Lauffenburger, D. A. Self-Assembly of a β -Sheet Protein Governed by Relief of Electrostatic Repulsion Relative to van der Waals Attraction. *Biomacromolecules* **2000**, *1*, 627–631.
- Savin, T.; Doyle, P. S. Electrostatic Tuned Rate of Peptide Self-Assembly Resolved by Multiple Particle Tracking. *Soft Matter* **2007**, *3*, 1194–1202.
- Tanaka, H.; Meunier, J.; Bonn, D. Nonergodic States of Charged Colloidal Suspension: Repulsive and Attractive Glasses and Gels. *Phys. Rev. E* **2004**, *69*, 031404.
- Bowerman, C. J.; Liyanage, W.; Federation, A. J.; Nilsson, B. L. Tuning β -Sheet Peptide Self-Assembly and Hydrogelation Behavior by Modification of Sequence Hydrophobicity and Aromaticity. *Biomacromolecules* **2011**, *12*, 2735–2745.
- Measey, T.; Schweitzer-Stenner, R. Aggregation of the Amphipathic Peptides (AAKA)_n into Antiparallel β Sheets. *J. Am. Chem. Soc.* **2006**, *128*, 13324–13325.
- Fauchere, J.-L.; Pliska, V. E. Hydrophobic Parameters of Amino Acid side Chains from the Partitioning of N-Acetyl-Amino Acid Amides. *Eur. J. Med. Chem.* **1983**, *18*, 369–375.
- Measey, T. J.; Schweitzer-Stenner, R.; Sa, V.; Kornev, K. Anomalous Conformational Instability and Hydrogel Formation of a Cationic Class of Self-Assembling Oligopeptides. *Macromolecules* **2010**, *43*, 7800–7806.
- Jang, S.; Yuan, J.-M.; Shin, J.; Measey, T. J.; Schweitzer-Stenner, R.; Li, F.-Y. Energy Landscape Associated with the Self-Aggregation of an Alanine-Based Oligopeptide. *J. Phys. Chem. B* **2009**, *113*, 6054–6061.

- (22) Sieler, G.; Schweitzer-Stenner, R. The Amide I Mode of Peptides in Aqueous Solution Involves Vibrational Coupling Between The Peptide Group and Water Molecules of The Hydration Shell. *J. Am. Chem. Soc.* **1997**, *119*, 1720–1726.
- (23) Jentzen, W.; Unger, E.; Karvounis, G.; Shelton, J. A.; Dreybrodt, W.; Schweitzer-Stenner, R. Conformational Properties of Nickel(II) Octaethylporphyrin in Solution. 1. Resonance Excitation Profiles and Temperature Dependence of Structure-Sensitive Raman Lines. *J. Phys. Chem.* **1996**, *100*, 14184–14191.
- (24) Schweitzer-Stenner, R. Simulated IR, Isotropic and Anisotropic Raman, and Vibrational Circular Dichroism Amide I Band Profiles of Stacked β -Sheets. *J. Phys. Chem. B* **2012**, *116*, 4141–4153.
- (25) Lee, C.; Cho, M. Local Amide I Mode Frequencies and Coupling Constants in Multiple-Stranded Antiparallel β -Sheet Polypeptides. *J. Phys. Chem. B* **2004**, *108*, 20397–20407.
- (26) Bour, P.; Keiderling, T. A. Structure, Spectra and the Effects of Twisting of β -Sheet Peptides. A Density Functional Theory Study. *J. Mol. Struct.: THEOCHEM* **2004**, *675*, 95–105.
- (27) Surewicz, W. K.; Mantsch, H. H. New Insight into Protein Secondary Structure from Resolution-Enhanced Infrared Spectra. *Biochim. Biophys. Acta, Protein Struct. Mol. Enzymol.* **1988**, *952*, 115–130.
- (28) Lee, S.-H.; Krimm, S. An Ab-Initio Based Vibrational Analysis of α -Poly(L-Alanine). *Biopolymers* **1998**, *46*, 283–317.
- (29) Chen, X. G.; Schweitzer-Stenner, R.; Asher, S. A.; Mirkin, N. G.; Krimm, S. Vibrational Assignments of trans-N-Methylacetamide and Some of Its Deuterated Isotopomers from Band Decomposition of IR, Visible, and Resonance Raman Spectra. *J. Phys. Chem.* **1995**, *99*, 3074–3083.
- (30) Han, W.-G.; Jalkanen, K. J.; Elstner, M.; Suhai, S. Theoretical Study of Aqueous N-Acetyl-L-Alanine N-Methylamide: Structures and Raman, VCD, and ROA Spectra. *J. Phys. Chem. B* **1998**, *102*, 2587–2602.
- (31) Schweitzer-Stenner, R.; Eker, F.; Huang, Q.; Griebenow, K.; Mroz, P. A.; Kozlowski, P. M. Structure Analysis of Di-peptides in Water by Exploring and Utilizing the Structural Sensitivity of Amide III by Polarized Visible Raman, FTIR-Spectroscopy and DFT Based Normal Coordinate Analysis. *J. Phys. Chem. B* **2002**, *106*, 4294–4304.
- (32) Numata, K.; Sato, R.; Yazawa, K.; Hikima, T.; Masunaga, H. Crystal Structure and Physical Properties of Antheraea Yamamai Silk Fibers: Long Poly(Alanine) Sequences are partially in the Crystalline Region. *Polymer* **2015**, *77*, 87–94.
- (33) Pérez, C.; Griebenow, K. Fourier-Transform Infrared Spectroscopic Investigation of The Thermal Denaturation of the Egg-White Lysozyme Dissolved in Aqueous Buffer and Glycerol. *Biotechnol. Lett.* **2000**, *22*, 1899–1905.
- (34) Krimm, S.; Bandekar, J. Vibrational Spectroscopy and Conformation of Peptides, Polypeptides, and Proteins. *Adv. Protein Chem.* **1986**, *38*, 181–364.
- (35) Kubelka, J.; Keiderling, T. A. Differentiation of β -Sheet-Forming Structures: Ab Initio-Based Simulations of IR Absorption and Vibrational CD for Model Peptide and Protein β -Sheets. *J. Am. Chem. Soc.* **2001**, *123*, 12048–12058.
- (36) Schweitzer-Stenner, R. Secondary Structure Analysis of Polypeptides Based on an Excitonic Coupling Model to Describe the Band Profile of Amide I of IR, Raman and Vibrational Circular Dichroism Spectra. *J. Phys. Chem. B* **2004**, *108*, 16965–16975.
- (37) Measey, T.; Schweitzer-Stenner, R. The Conformations Adopted by the Octamer Peptide (AAKA)₂ in Aqueous Solution probed by FTIR and Polarized Raman Spectroscopy. *J. Raman Spectrosc.* **2006**, *37*, 248–254.
- (38) Measey, T. J.; Schweitzer-Stenner, R. Vibrational Circular Dichroism as a Probe of Fibrillogenesis: The Origin of the Anomalous Intensity Enhancement of Amyloid-like Fibrils. *J. Am. Chem. Soc.* **2011**, *133*, 1066–1076.
- (39) Javid, N.; Roy, S.; Zelzer, M.; Yang, Z.; Sefcik, J.; Ulijn, R. V. Cooperative Self-Assembly of Peptide Gelators and Proteins. *Biomacromolecules* **2013**, *14*, 4368–4376.
- (40) Schneider, J. P.; Pochan, D. J.; Ozbas, B.; Rajagopal, K.; Pakstis, L.; Kretsinger, J. Responsive Hydrogels from the Intramolecular Folding and Self-Assembly of a Designed Peptide. *J. Am. Chem. Soc.* **2002**, *124* (50), 15030–15037.
- (41) Fung, S. Y.; Keyes, C.; Duhamel, J.; Chen, P. Concentration Effect on the Aggregation of a Self-Assembling Oligopeptide. *Biophys. J.* **2003**, *85*, 537–548.
- (42) Thompson, M. J.; Sievers, S. A.; Karanicolas, J.; Ivanova, M. I.; Baker, D.; Eisenberg, D. The 3D profile method for identifying fibril-forming segments of proteins. *Proc. Natl. Acad. Sci. U. S. A.* **2006**, *103*, 4074–4078.
- (43) Kundu, S. K.; Yoshida, M.; Shibayama, M. Effect of Salt Content on the Rheological Properties of Hydrogel Based on Oligomeric Electrolyte. *J. Phys. Chem. B* **2010**, *114*, 1541–1547.
- (44) Manas, E. S.; Getahun, Z.; Wright, W. W.; DeGrado, W. F.; Vanderkooi, J. M. Infrared Spectra of Amide Groups in α -Helical Proteins: Evidence for Hydrogen Bonding between Helices and Water. *J. Am. Chem. Soc.* **2000**, *122*, 9883–9890.
- (45) Ackels, L.; Stawski, P.; Amunson, K. E.; Kubelka, J. On the Temperature Dependence of Amide I Intensities of Peptides in Solution. *Vib. Spectrosc.* **2009**, *50*, 2–9.
- (46) Huggins, D. J. Benchmarking the Thermodynamic Analysis of Water Molecules Around a Model Beta Sheet. *J. Comput. Chem.* **2012**, *33*, 1383–1392.
- (47) Riter, R. E.; Willard, D. M.; Levinger, N. E. Water Immobilization at Surfactant Interfaces in Reverse Micelles. *J. Phys. Chem. B* **1998**, *102*, 2705–2714.